

Supplementary Information

Growth Mechanism and Active Sites Probing of Fe₃C@N-doped Carbon Nanotubes/C Catalysts: Guidance for Building Highly Efficient Oxygen Reduction Electrocatalysts

**Jianbing Zhu^{ab}, Meiling Xiao^{ab}, Changpeng Liu^c, Junjie Ge^{d*}, Jean St-Pierre^{d*} and
Wei Xing^{a,c,*}**

^aState Key Laboratory of Electroanalytical Chemistry, Changchun Institute of Applied Chemistry, Chinese Academy of Sciences, Changchun, Jilin, 130022, China.

^bGraduate School of the Chinese Academy of Sciences, Beijing, 100039, China

^cLaboratory of Advanced Power Sources, Changchun Institute of Applied Chemistry, Changchun, 130022, PR China

Address: 5625 Renmin Street, Changchun 130022, PR China

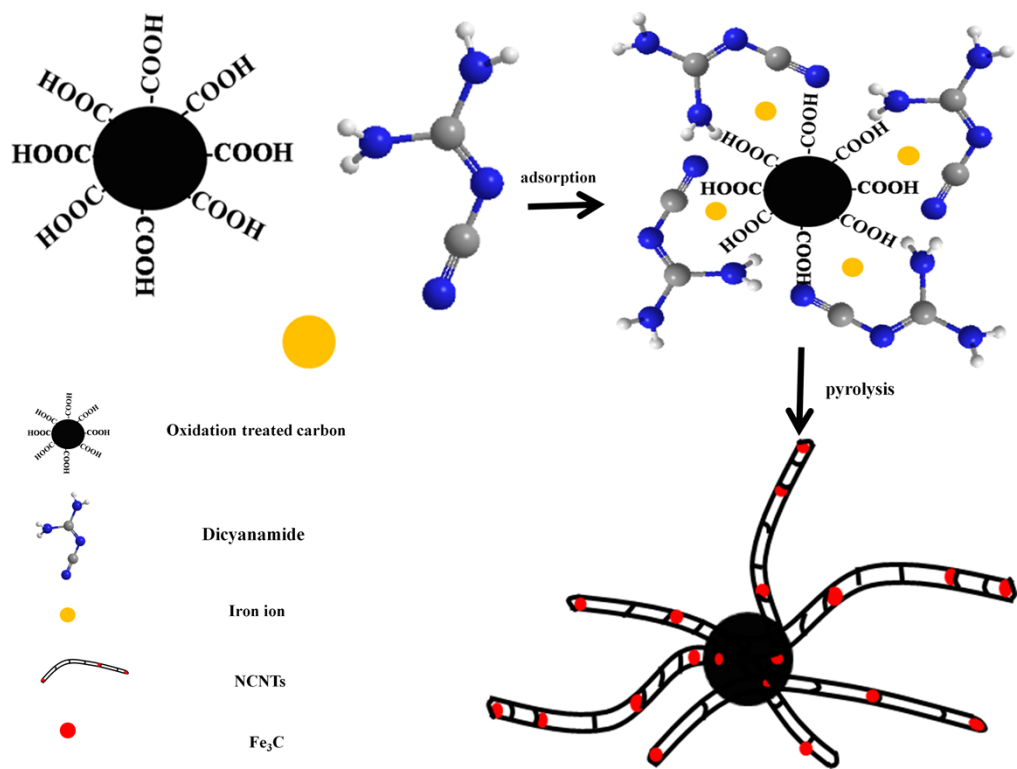
^dHawaii Natural Energy Institute, University of Hawaii

Address: Manoa, 1680 East-West Road, POST 109, Honolulu, HI 96822, USA

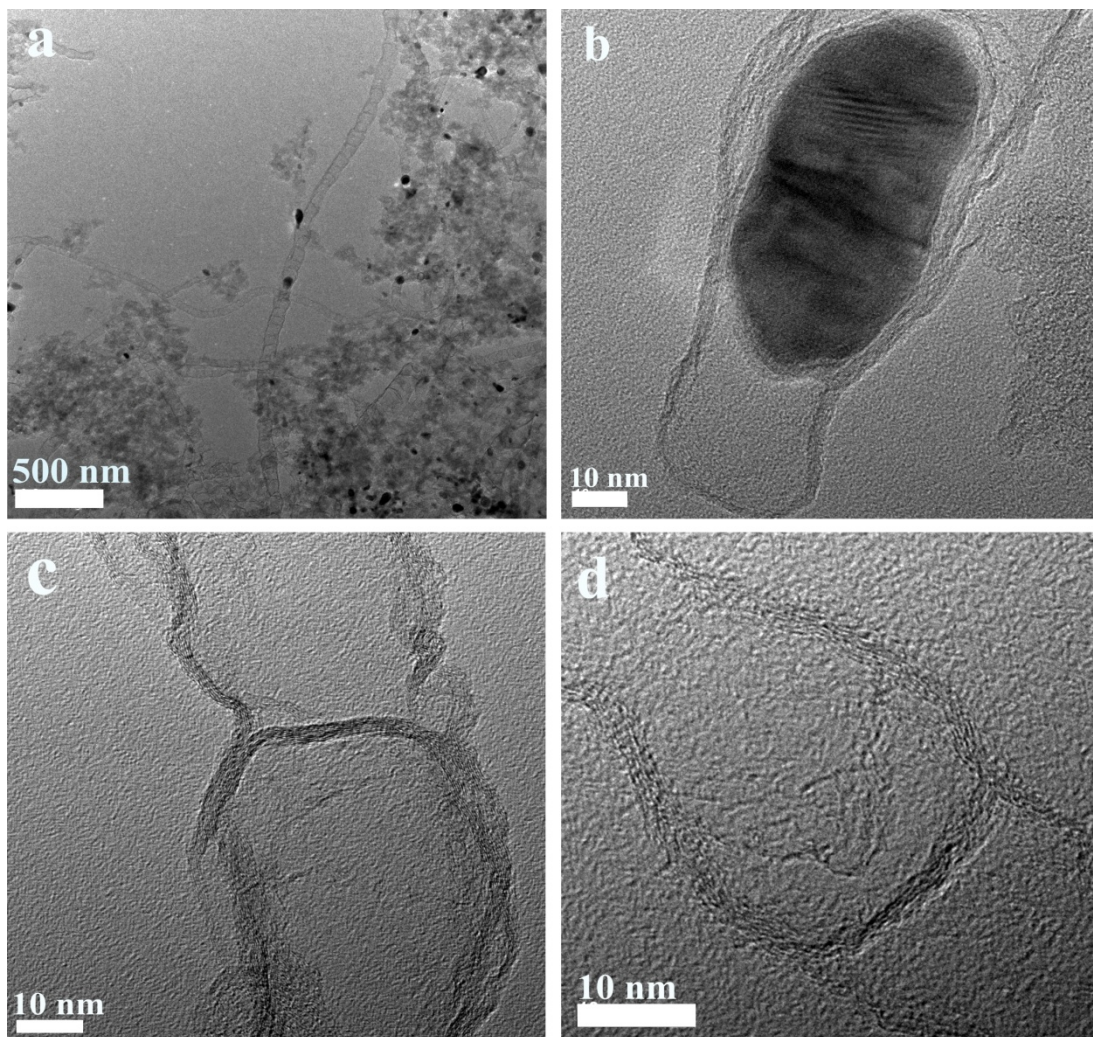
E-mail Address: xingwei@ciac.jl.cn; gejunjie@hawaii.edu and jsp7@hawaii.edu

Tel: +86-431-85262223

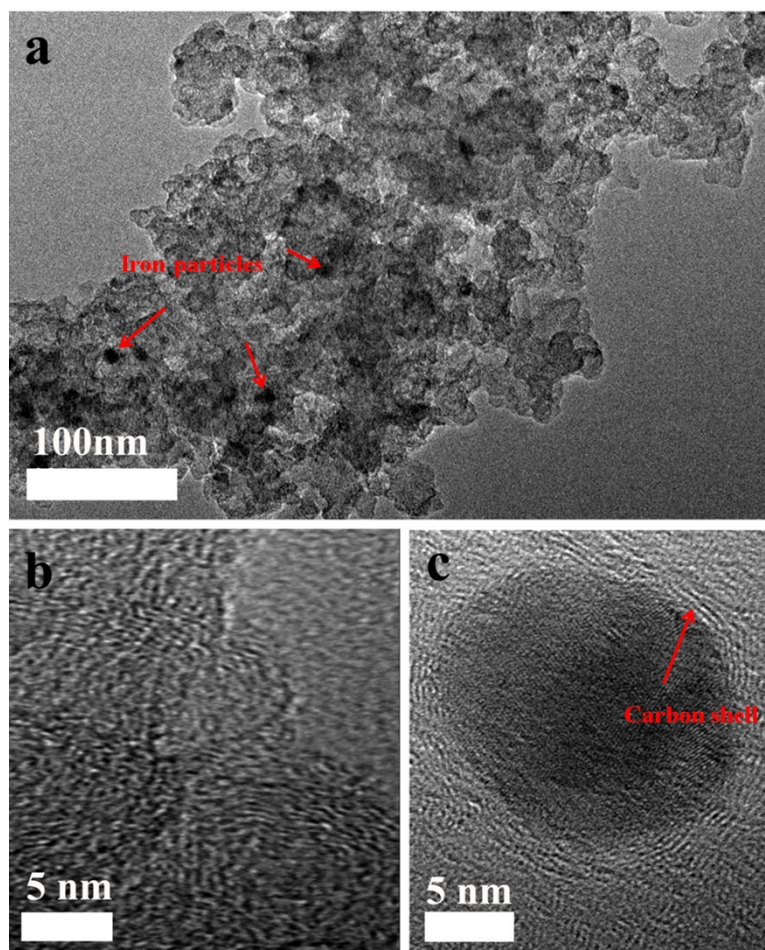
Fax: +86-431-85685653



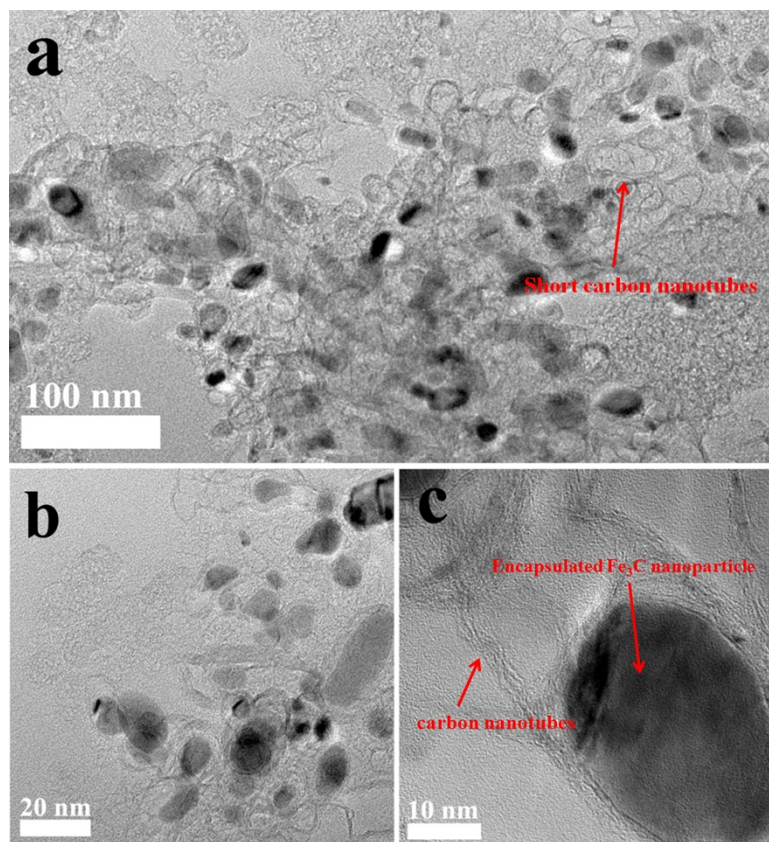
Supplementary Scheme S1. Schematic view of the synthesis of the $Fe_3C/NCNTs/OBP$ catalysts.



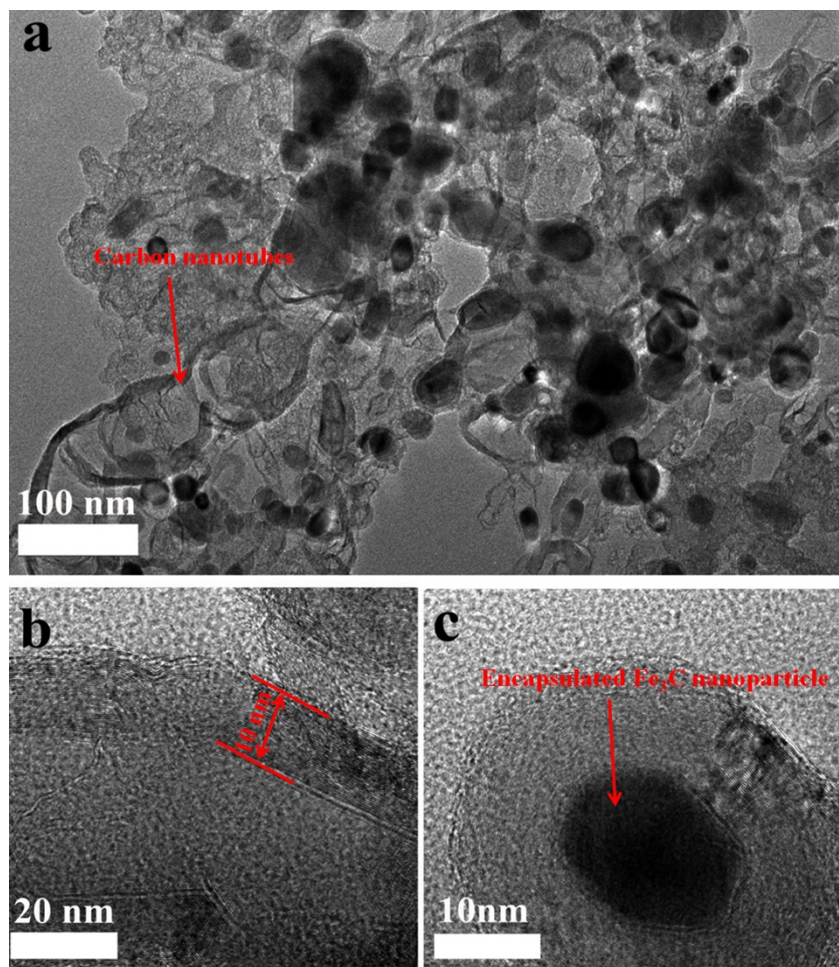
Supplementary Figure S1. TEM images for Fe₃C/NCNTs/OBP-900 catalyst at different magnifications.



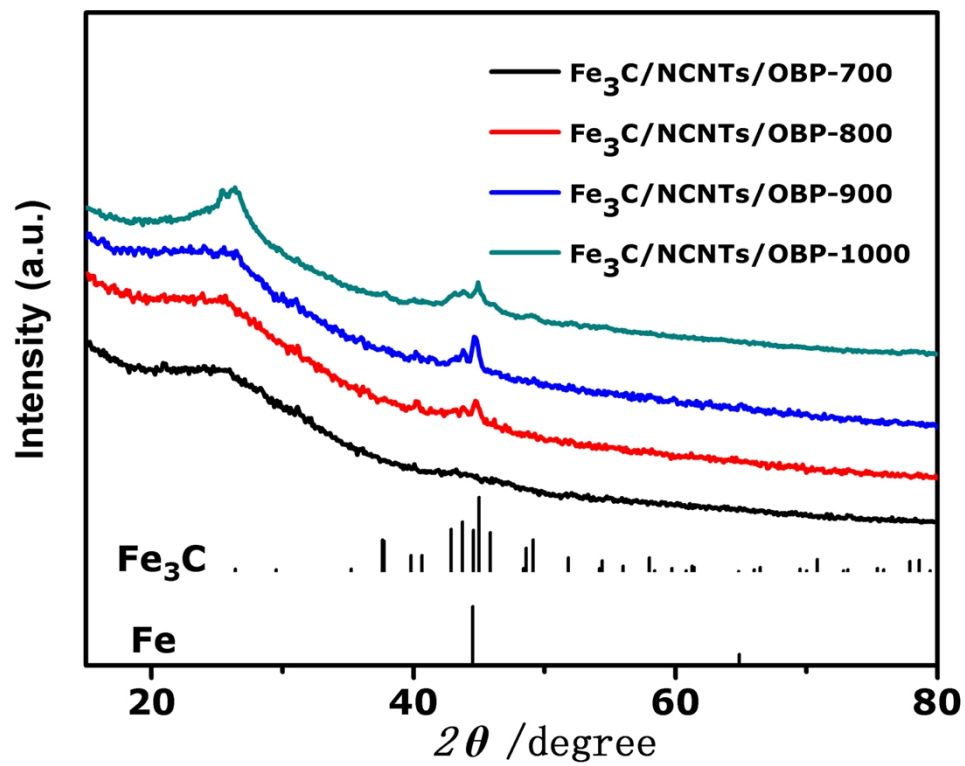
Supplementary Figure S2. TEM images showing the morphology of $\text{Fe}_3\text{C}/\text{NCNTs}/\text{OBP-700}$ catalyst, no obvious CNTs was observed from the composite, hollow structure formed by graphitic carbon layers and nanoparticles encapsulated in several carbon nanoshells on the edges of the catalyst were found by HRTEM.



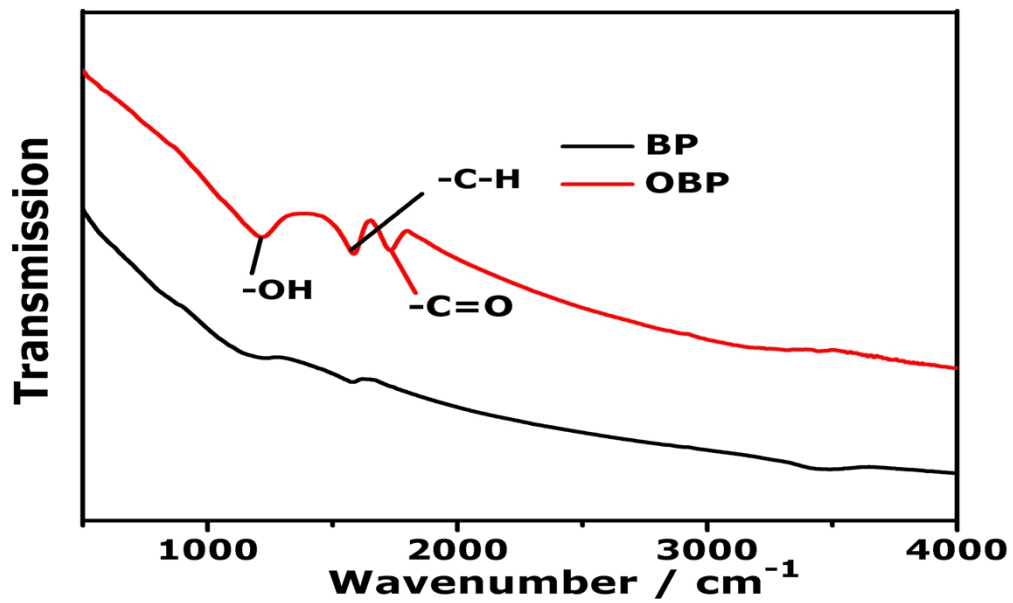
Supplementary Figure S3. TEM images of Fe₃C/NCNTs/OBP-800 catalyst, bamboo-like CNTs with anomalous carbon structure encapsulated Fe/Fe₃C was observed in the composite, hollow structure formed by graphitic carbon layers and nanoparticles encapsulated in several carbon nanoshells on the edges of the catalyst were found by HRTEM.



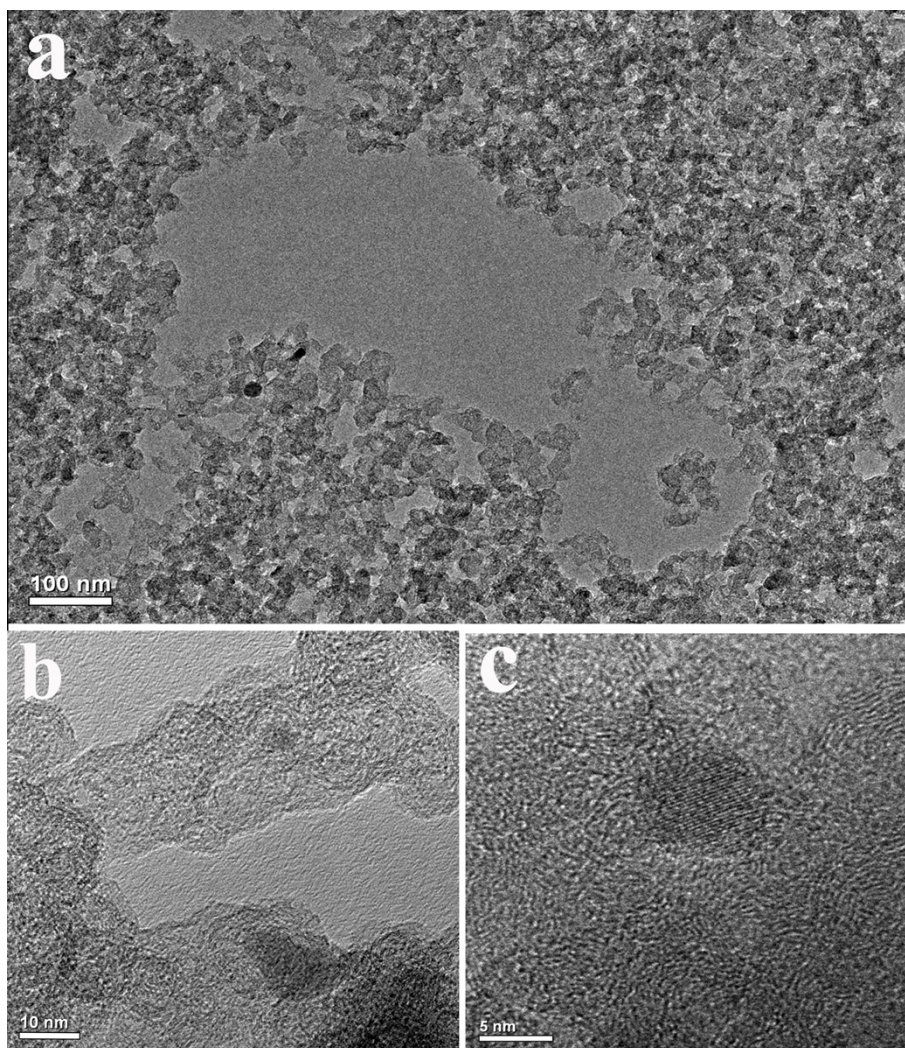
Supplementary Figure S4. TEM images of Fe₃C/NCNTs/OBP-1000 catalyst, CNTs with much more wall thickness and Fe₃C nanoparticle encapsulated in thick carbon layer is observed.



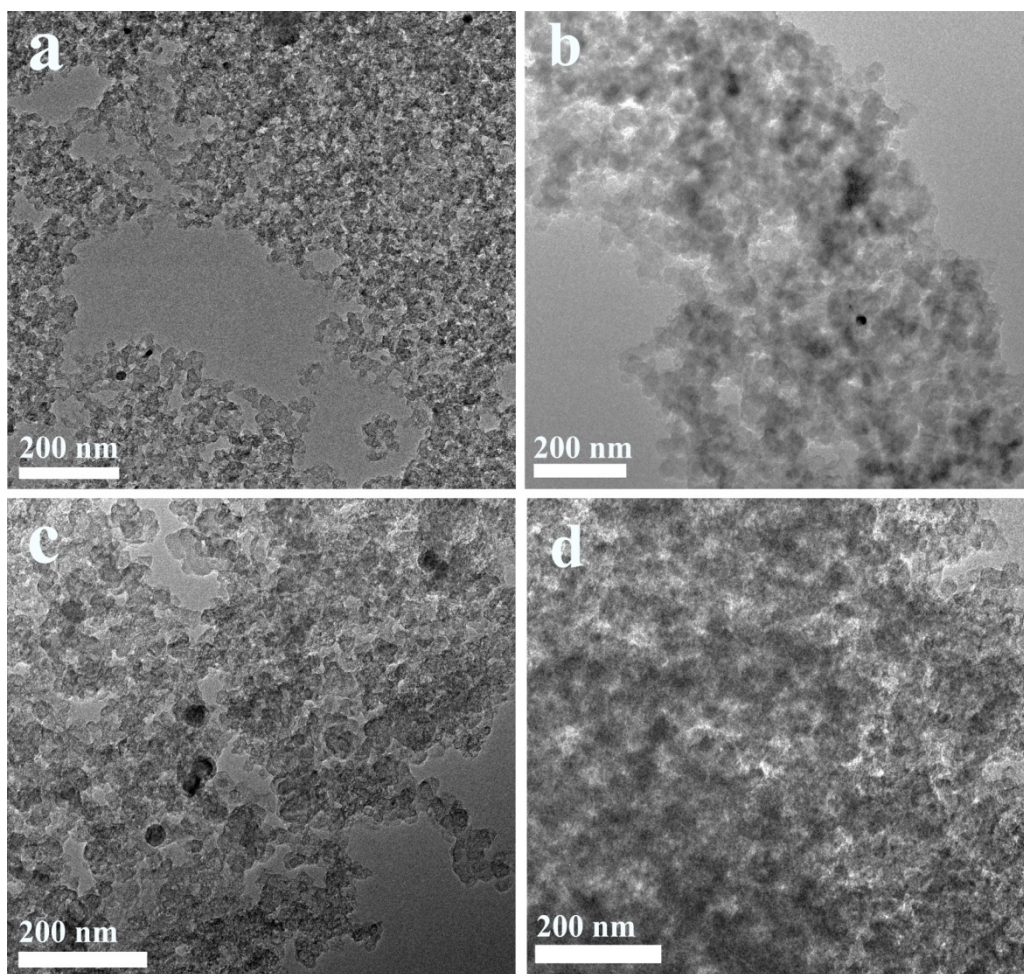
Supplementary Figure S5. XRD spectra of the Fe₃C/NCNTs/OBP catalysts pyrolyzed at different temperatures.



Supplementary Figure S6. FT-IR spectra of the oxidized BP-2000 and pure BP-2000 (BP).



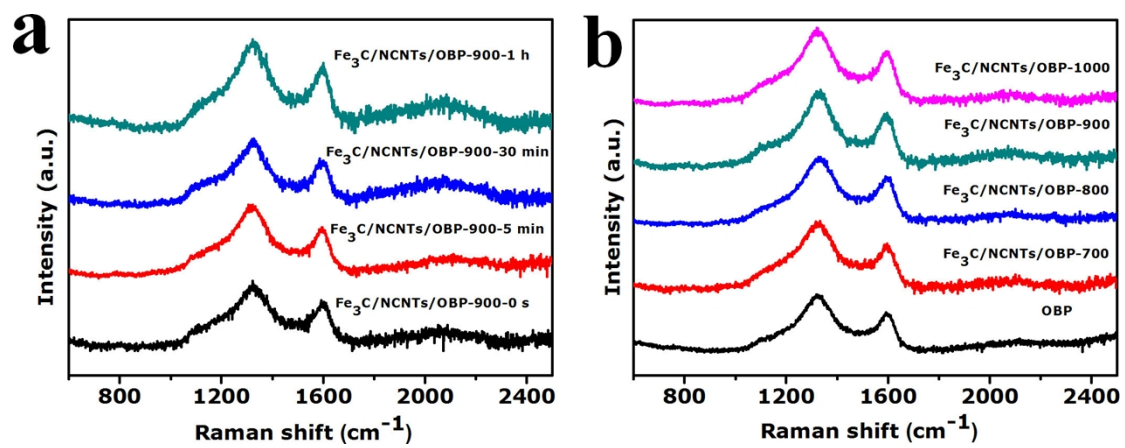
Supplementary Figure S7. TEM images for the Fe₃C/NC/BP-900 catalyst at different magnifications.



Supplementary Figure S8. Catalysts derived from carbon substrates without oxidation treatment,

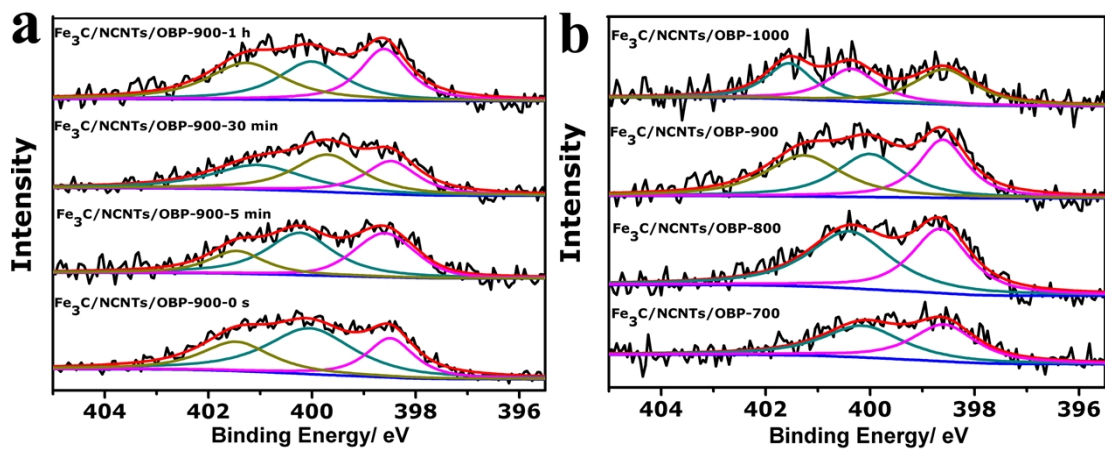
(a) black Pearls® 2000 carbon black (b) vulcan XC-72R carbon black; (c) acetylene carbon black;

(d) vulcan XC-72 carbon black.

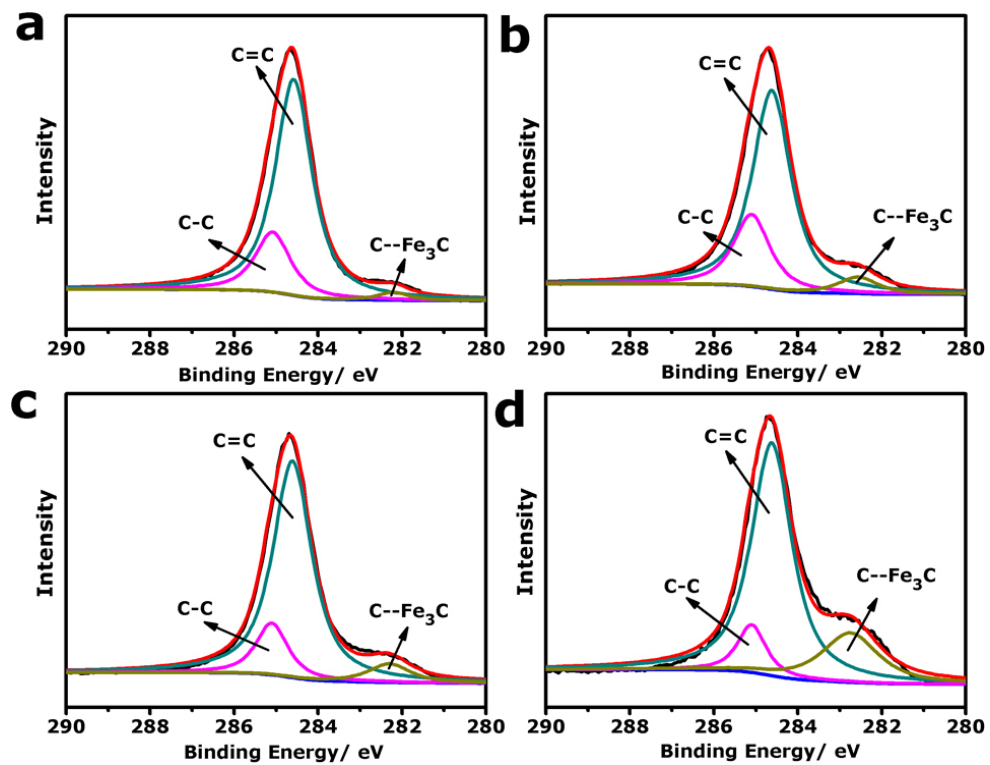


Supplementary Figure S9. Raman spectra of the catalysts synthesized with different conditions.

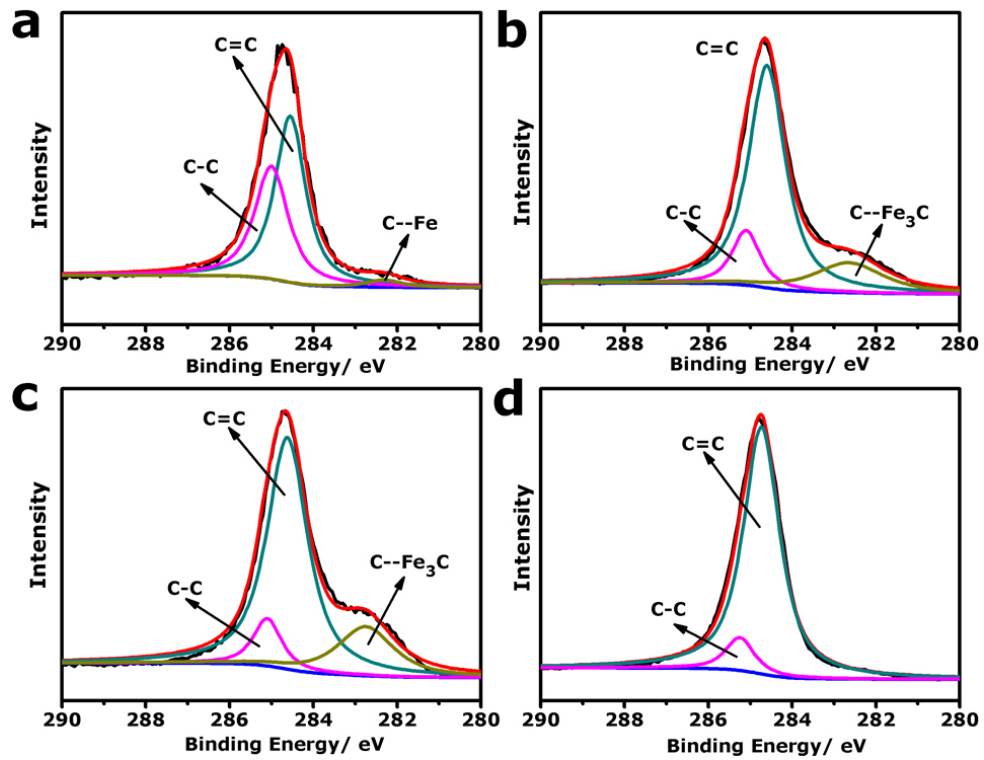
(a) Fe₃C/NCNTs/OBP catalysts pyrolyzed at 900 °C with different time; (b) OBP and catalysts pyrolyzed at different temperatures.



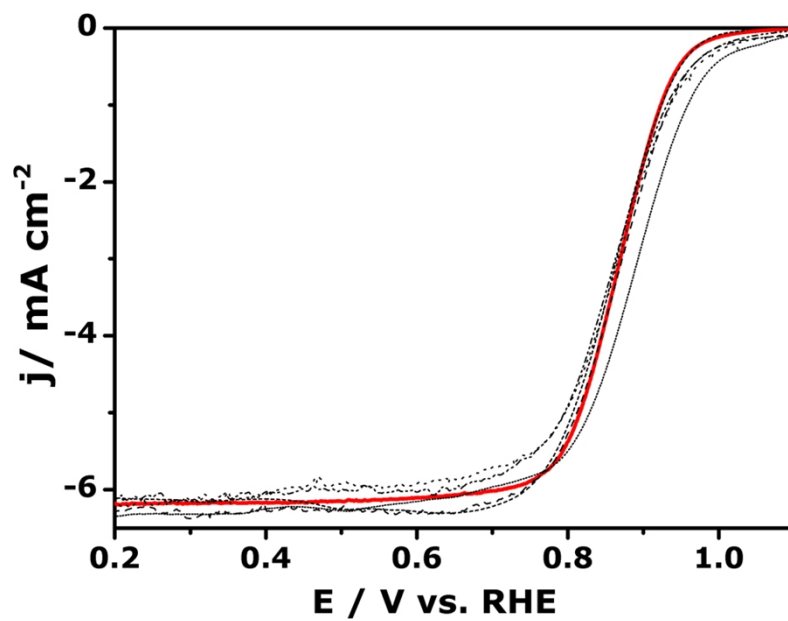
Supplementary Figure S10. High resolution N 1s spectra from XPS. (a) The Fe₃C/NCNTs/OBP catalysts pyrolyzed at 900 °C with different time; (b) catalysts pyrolyzed at different temperatures.



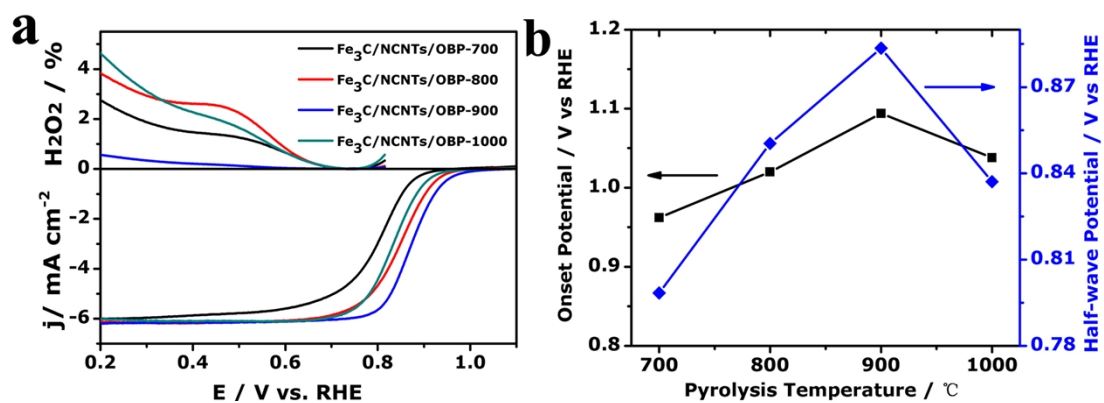
Supplementary Figure 11. High resolution XPS spectra of C 1s of Fe₃C/NCNTs/OBP catalysts pyrolyzed at 900 °C with different time; (a) 0 s; (b) 5 min; (c) 30 min and (d) 1h.



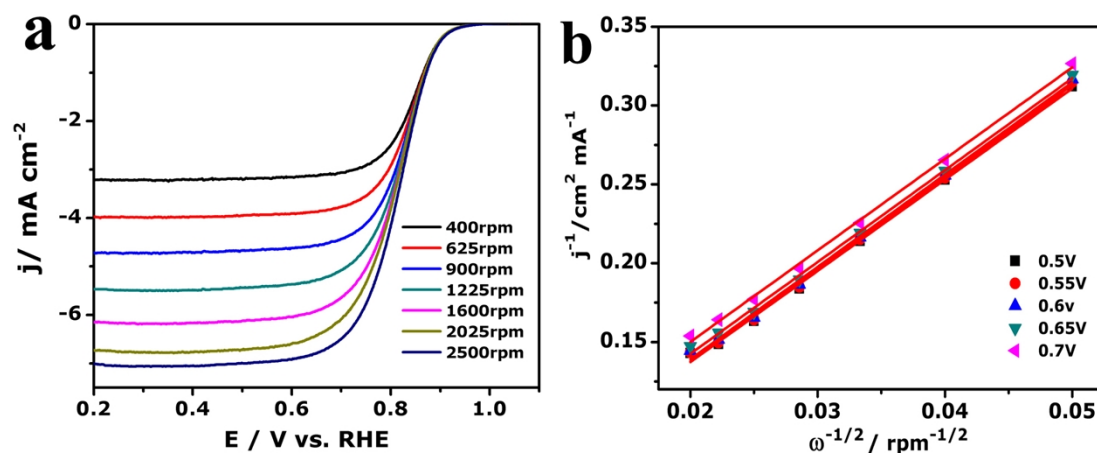
Supplementary Figure 12. High resolution XPS spectra of C 1s of $\text{Fe}_3\text{C}/\text{NCNTs}/\text{OBP}$ catalysts pyrolyzed at different temperatures; (a) $\text{Fe}_3\text{C}/\text{NCNTs}/\text{OBP}$ -700, (b) $\text{Fe}_3\text{C}/\text{NCNTs}/\text{OBP}$ -800, (c) $\text{Fe}_3\text{C}/\text{NCNTs}/\text{OBP}$ -900 and (d) $\text{Fe}_3\text{C}/\text{NCNTs}/\text{OBP}$ -1000.



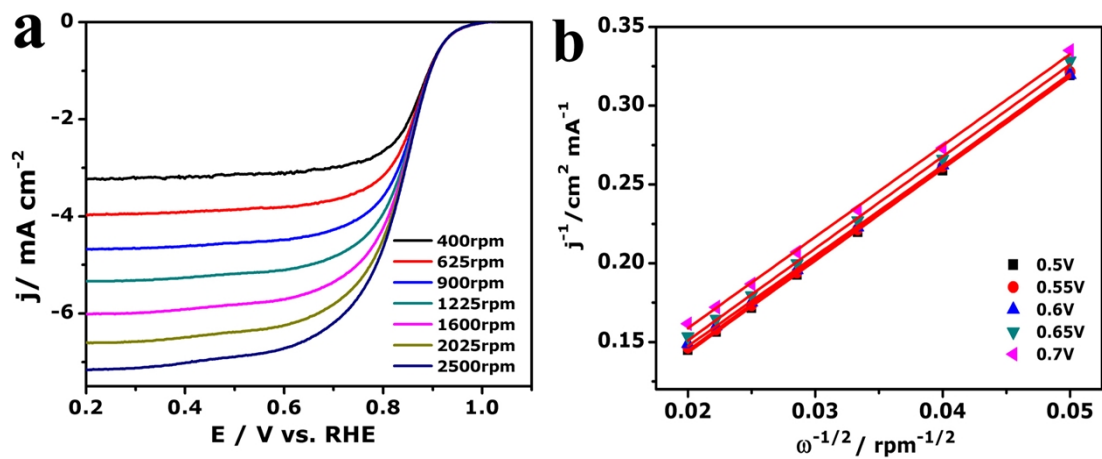
Supplementary Figure 13. RDE polarization curves plots recorded with $\text{Fe}_3\text{C/NCNTs/OBP-900}$ catalysts from six different syntheses. Curve in red has been used in Fig. 3a in the manuscript.



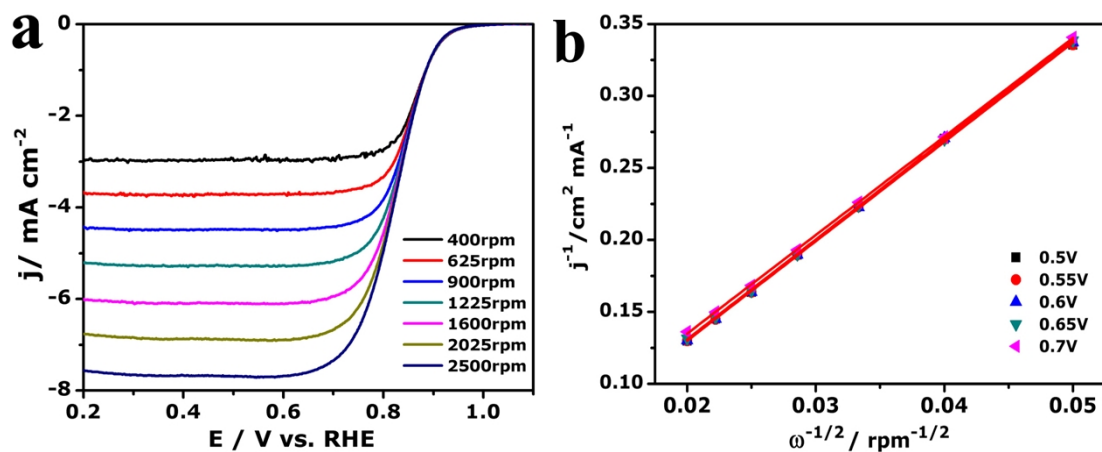
Supplementary Figure S14. (a) Linear sweep voltammetry for oxygen reduction on $\text{Fe}_3\text{C}/\text{NCNTs}/\text{OBP}$ catalysts pyrolyzed at different temperatures in O_2 -saturated 0.1 M KOH at 1600 rpm with scan rate of 5 mV/s, (b) the onset and half-wave potential evolves with the pyrolysis temperature.



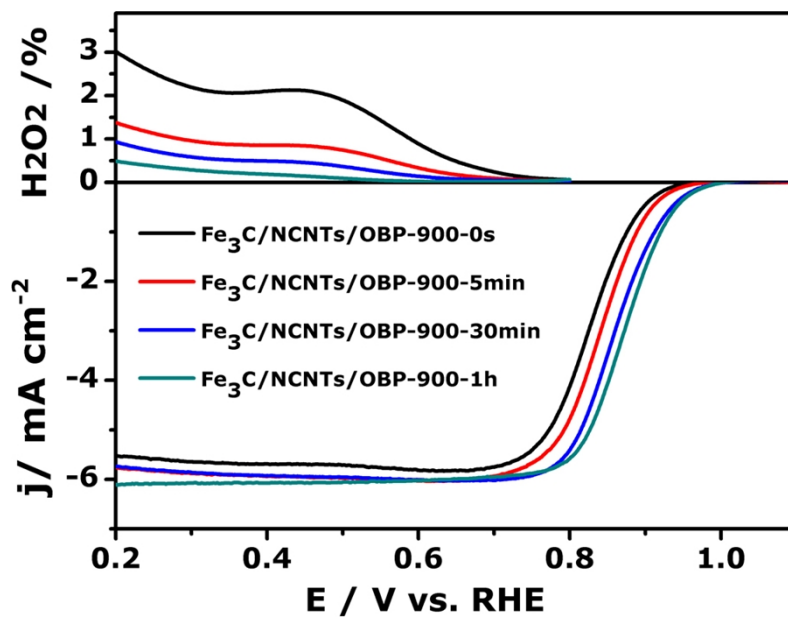
Supplementary Figure S15. (a) Linear sweep voltammetry for oxygen reduction at the $\text{Fe}_3\text{C}/\text{NCNTs}/\text{OBP-700}$ catalyst in O_2 -saturated 0.1 M KOH under various rotation speeds at scan rate of 5 mV/s, (b) K-L plots at different potentials.



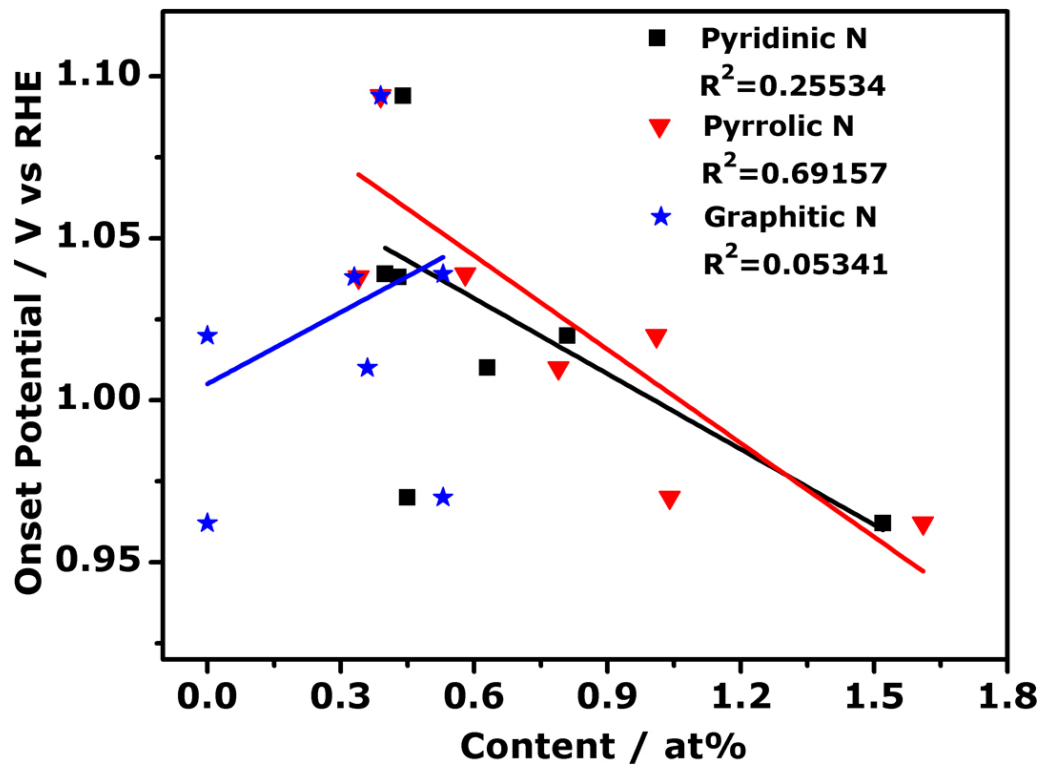
Supplementary Figure S16. (a) Linear sweep voltammetry for oxygen reduction on the $\text{Fe}_3\text{C}/\text{NCNTs}/\text{OBP-800}$ catalyst in O_2 -saturated 0.1 M KOH under various rotation speeds at scan rate of 5 mV/s, (b) K-L plots at different potentials.



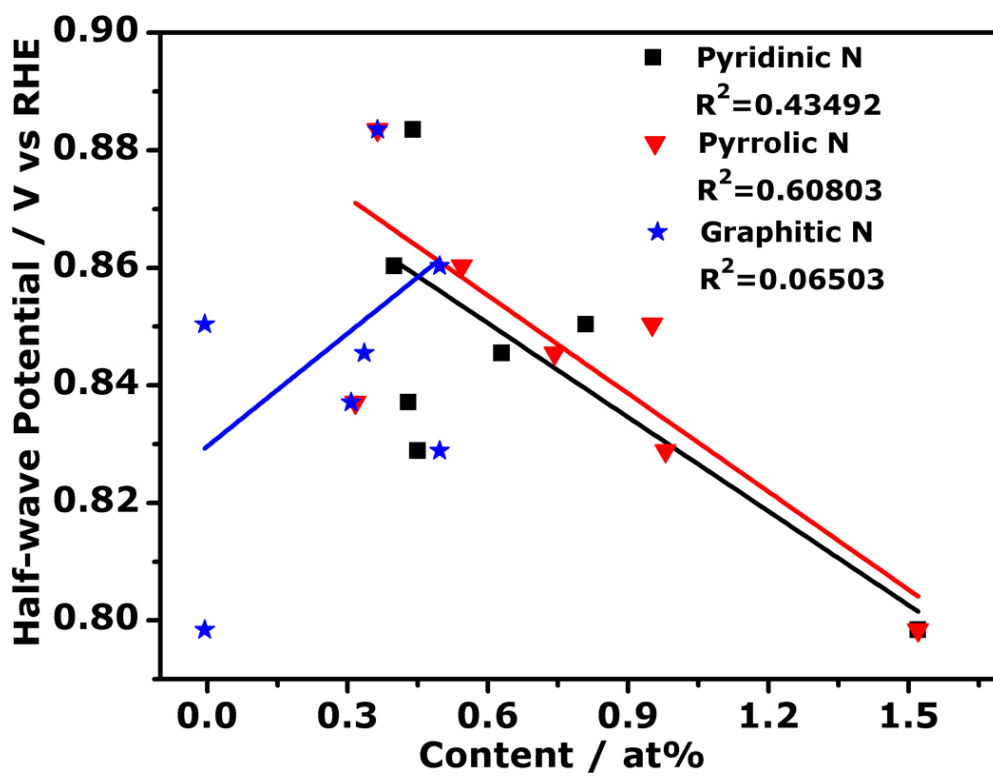
Supplementary Figure S17. (a) Linear sweep voltammetry for oxygen reduction on $\text{Fe}_3\text{C}/\text{NCNTs}/\text{OBP-1000}$ catalyst in O_2 -saturated 0.1 M KOH under various rotation speeds at scan rate of 5 mV/s, (b) K-L plots at different potentials.



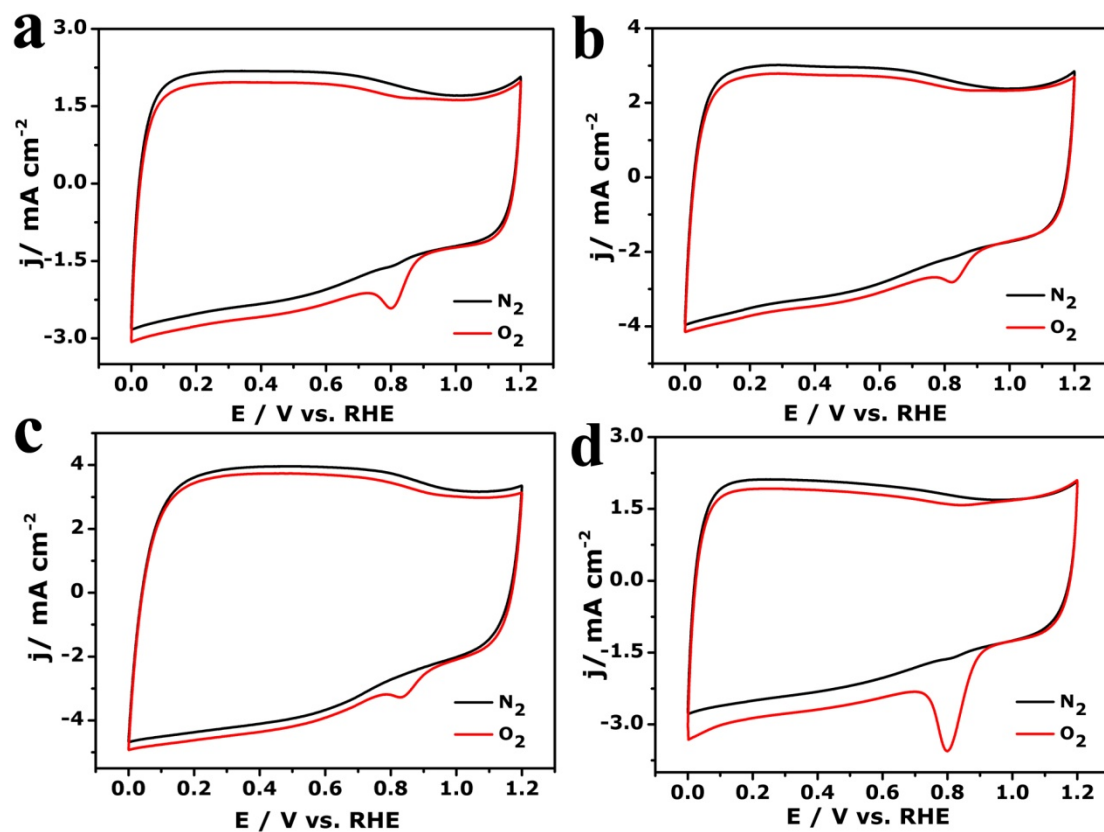
Supplementary Figure S18. Linear sweep voltammetry for oxygen reduction on Fe₃C/NCNTs/OBP catalysts pyrolyzed at 900 °C with different time in O₂-saturated 0.1 M KOH under 1600 rpm at scan rate of 5 mV/s and the corresponding H₂O₂ yielding.



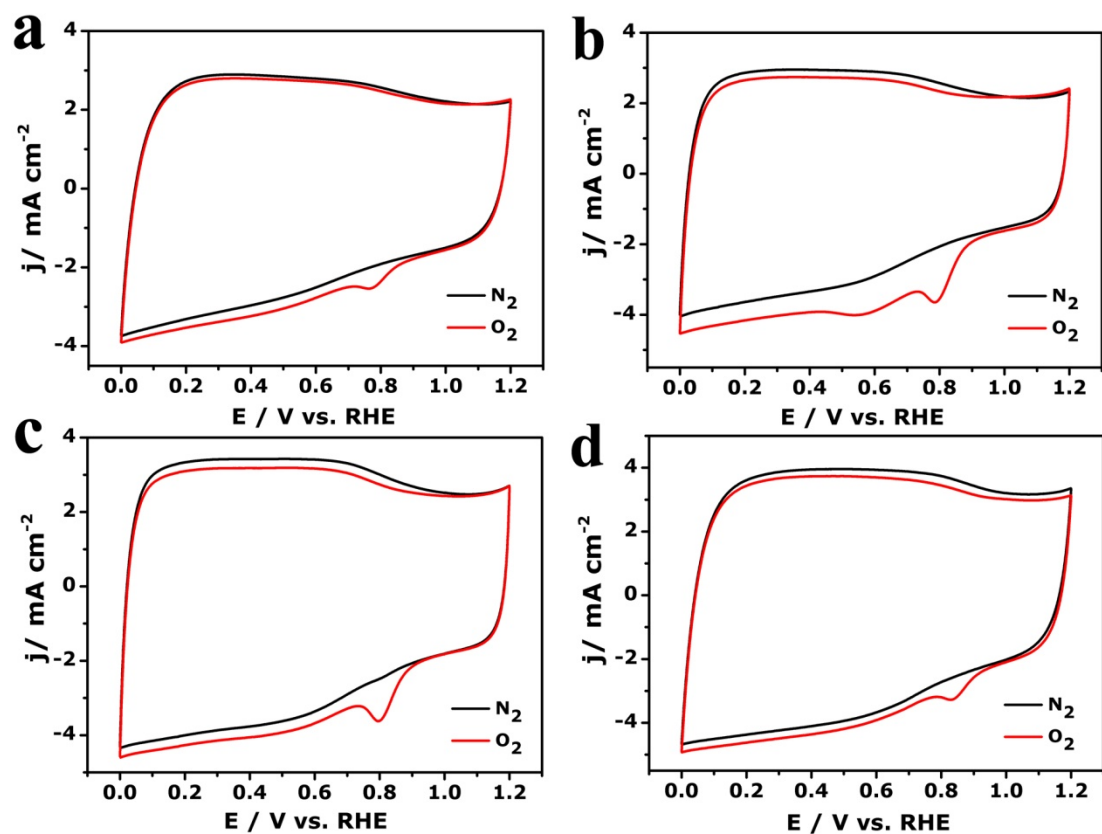
Supplementary Figure 19. Atomic % of pyridinic N, pyrrolic N and graphitic N versus onset potential of Fe₃C/NCNTs/OBP catalysts heattreated at various temperatures and time.



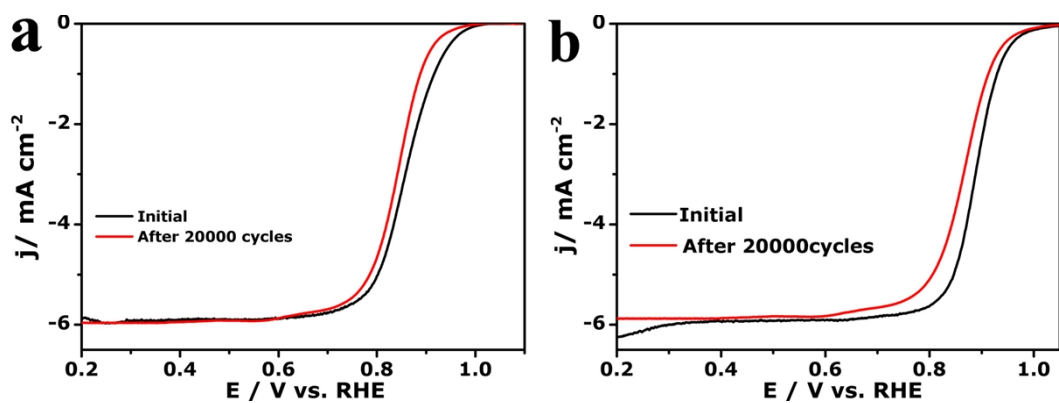
Supplementary Figure 20. Atomic % of pyridinic N, pyrrolic N and graphitic N versus half-wave potential of Fe₃C/NCNTs/OBP catalysts heattreated at various temperatures and time.



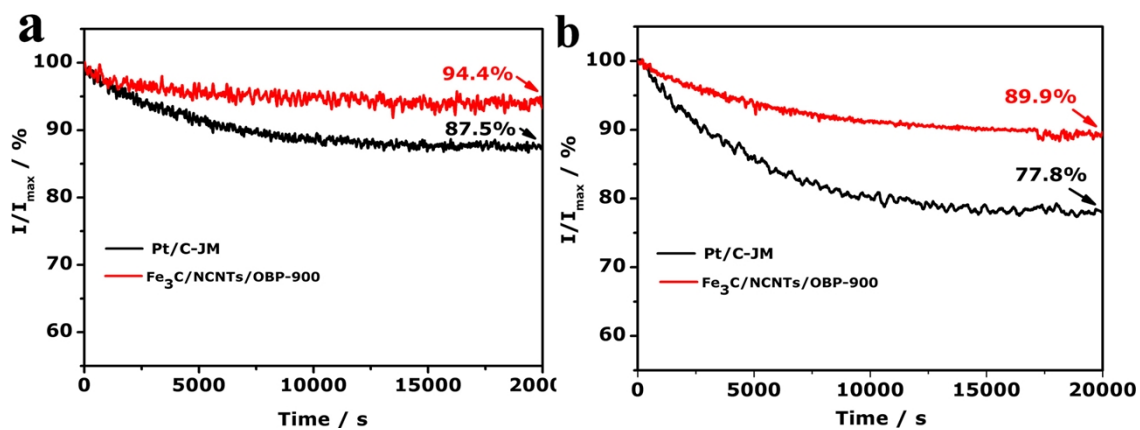
Supplementary Figure 21. CV curves of $\text{Fe}_3\text{C/NCNTs/OBP}$ in N_2 - (black line) or O_2 -saturated (red line) solution with a scan rate of 50 mVs^{-1} ; (a) $\text{Fe}_3\text{C/NCNTs/OBP-700}$, (b) $\text{Fe}_3\text{C/NCNTs/OBP-800}$, (c) $\text{Fe}_3\text{C/NCNTs/OBP-900}$ and (d) $\text{Fe}_3\text{C/NCNTs/OBP-1000}$.



Supplementary Figure 22. CV curves of $\text{Fe}_3\text{C/NCNTs/OBP-900}$ in N_2 - (black line) or O_2 -saturated (red line) solution with a scan rate of 50 mVs^{-1} ; (a) $\text{Fe}_3\text{C/NCNTs/OBP-900-0s}$, (b) $\text{Fe}_3\text{C/NCNTs/OBP-900-5min}$, (c) $\text{Fe}_3\text{C/NCNTs/OBP-900-30min}$ and (d) $\text{Fe}_3\text{C/NCNTs/OBP-900-1h}$.



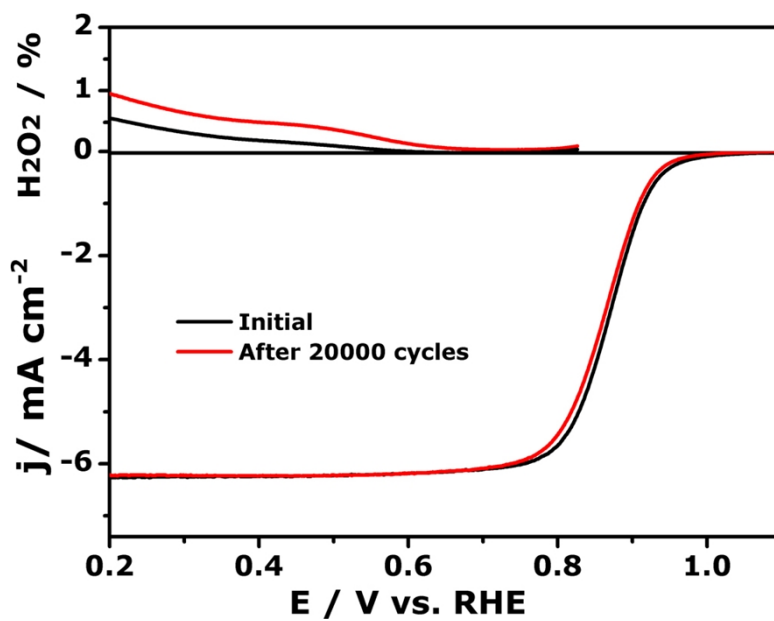
Supplementary Figure S23. RDE polarization curves for oxygen reduction on Pt/C-JM catalyst at 1600 rpm in O₂-saturated (a) 0.1 M KOH and (b) 0.1M HClO₄ at scan rate of 5 mV s⁻¹ before and after 20,000 cycles test.



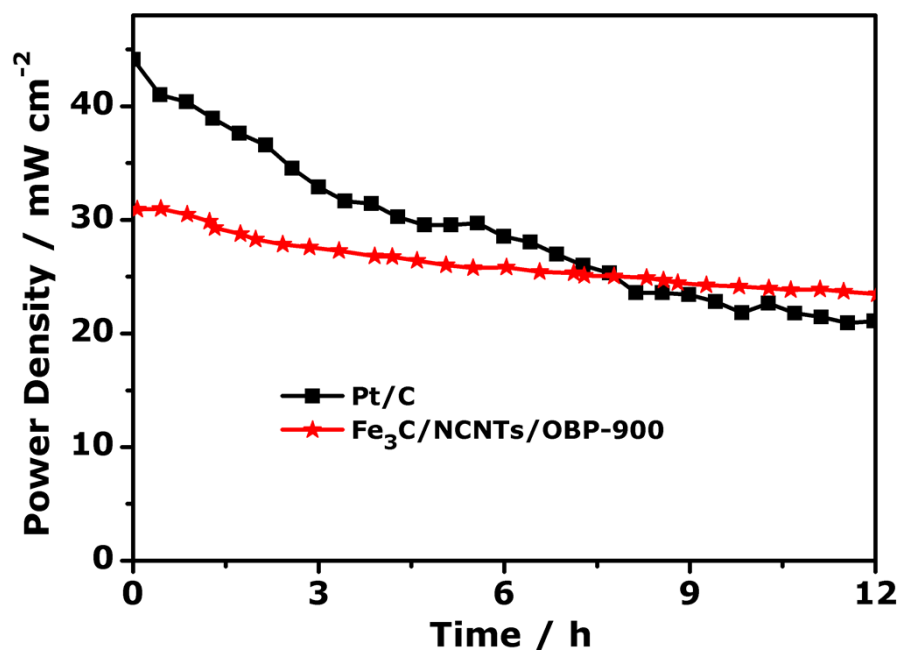
Supplementary Figure S24. Chronoamperometric measurement of Fe₃C/NCNTs/OBP-900 and

Pt/C-JM catalysts at 1600 rpm in O₂-saturated solution (a) 0.1 M KOH and (b) 0.1M HClO₄, the

potential is held at 0.8V.



Supplementary Figure S25. RDE polarization curves and peroxide yield of Fe₃C/NCNTs/OBP-900 O₂-saturated 0.1 M KOH before and after ADT test at scan rate of 5 mV s⁻¹ and rotation speed of 1600 rpm.



Supplementary Figure S26. The discharge curves at 0.2 V for direct methanol fuel cells employing $\text{Fe}_3\text{C/NCNTs/OBP-900}$, Pt/C-20% as cathode and PtRu/C-30% as anode catalysts. Conditions: 1 M methanol at 60 °C. The flowing rate of methanol was 10 mL min^{-1} and the flowing rate of O_2 was 200 mL min^{-1}

Supplementary Table S1 The element composition for the synthesized catalysts

Sample	atomic content / %						
	C ^a	O ^a	N ^a	Fe ^a	Fe ^b	Mn ^a	Mn ^b
BP-2000	93.68	6.32	NA	NA	NA	NA	NA
OBP	90.84	9.12	NA	NA	0.01	NA	0.03
Fe ₃ C/N/BP-900	94.72	4.09	0.93	0.26	0.41	NA	NA
Fe ₃ C/NCNTs/OBP - 700	92.3	4.57	3.13	NA	1.35	NA	0.023
Fe ₃ C/NCNTs/OBP - 800	92.79	5.18	1.83	0.21	1.67	NA	0.035
Fe ₃ C/NCNTs/OBP - 900	94.99	3.79	1.22	NA	2.14	NA	0.029
Fe ₃ C/NCNTs/OBP - 1000	94.3	4.6	1.1	NA	1.93	NA	0.033

^{a)} Derived from XPS; ^{b)} ICP-OES and the metal content is normalized to mass fraction.

Supplementary Table S2 The nitrogen content and nitrogen type of the catalysts synthesized at different temperature

Sample	atomic content / %			
	Total N	pyridinic N	pyrrolic N	graphitic N
Fe ₃ C/NCNTs/OBP-700	3.13	1.52	1.61	-
Fe ₃ C/NCNTs/OBP-800	1.82	0.81	1.01	-
Fe ₃ C/NCNTs/OBP-900	1.22	0.44	0.39	0.39
Fe ₃ C/NCNTs/OBP-1000	1.1	0.43	0.34	0.33

Supplementary Table S3 The nitrogen content and nitrogen type of samples pyrolyzed at 900 °C with different time and quenching to room temperature

Sample	atomic content / %			
	Total N	pyridinic N	pyrrolic N	graphitic N
Fe ₃ C/NCNTs/OBP - 900-0s	2.05	0.45	1.04	0.53
Fe ₃ C/NCNTs/OBP - 900-5 min	1.78	0.63	0.79	0.36
Fe ₃ C/NCNTs/OBP - 900-30 min	1.51	0.40	0.58	0.53
Fe ₃ C/NCNTs/OBP - 900-1h	1.22	0.44	0.39	0.39

Supplementary Table S4 The calculated value of I_D/I_G from Raman spectra

Sample	I_D/I_G
OBP	3.52
Fe ₃ C/NCNTs/OBP -700	3.27
Fe ₃ C/NCNTs/OBP -800	2.84
Fe ₃ C/NCNTs/OBP -900	2.43
Fe ₃ C/NCNTs/OBP -1000	2.25
Fe ₃ C/NCNTs/OBP - 900-0s	2.73
Fe ₃ C/NCNTs/OBP - 900-5 min	2.63
Fe ₃ C/NCNTs/OBP - 900-30 min	2.51

References

- 1 Liang, Y. *et al.* Co₃O₄ nanocrystals on graphene as a synergistic catalyst for oxygen reduction reaction. *Nature materials* **10**, 780-786 (2011).
- 2 Hummers Jr, W. S. & Offeman, R. E. Preparation of graphitic oxide. *Journal of the American Chemical Society* **80**, 1339-1339 (1958).
- 3 Wang, S., Yu, D., Dai, L., Chang, D. W. & Baek, J.-B. Polyelectrolyte-Functionalized Graphene as Metal-Free Electrocatalysts for Oxygen Reduction. *ACS Nano* **5**, 6202-6209, doi:10.1021/nn200879h (2011).